

SUBMILLIMETER OBSERVATIONS OF W3

D. T. JAFFE,¹ R. H. HILDEBRAND,¹ JOCELYN KEENE,¹ AND S. E. WHITCOMB¹

Enrico Fermi Institute, University of Chicago

Received 1983 April 22; accepted 1983 June 21

ABSTRACT

We present a 35'' resolution, 400 μm continuum map of the core of the W3 molecular cloud complex. The map shows prominent peaks centered approximately at the positions of the infrared sources IRS 4 and IRS 5 with stronger emission at the western (IRS 4) peak. The visual extinction (inferred from the submillimeter measurements) through the center of both peaks is large ($A_v \sim 200$). We estimate a total mass for the core of 900 M_\odot , consistent with dynamical estimates if the observed velocity gradient is a result of rotation. The peak H_2 density is approximately $2.8 \times 10^5 \text{ cm}^{-3}$. The observations exclude the possibility that the shell H II regions, W3A–C, could be in pressure equilibrium with the surrounding cloud. The observations establish that the core of W3 contains several massive condensations surrounding the youngest stars in the region.

Subject headings: infrared: sources — interstellar: matter

I. INTRODUCTION

The core of the W3 complex contains a variety of objects in different stages of evolution within a 2' by 3' area (1.2 by 1.8 pc at 2 kpc). Figure 1 (adapted from Colley 1980) shows the spatial relation of these objects. The various objects include a well-developed shell H II region (W3A), several compact shell H II regions (W3B, W3C), and several ultracompact H II regions (W3F, W3M; near W3 IRS 7 and IRS 5, respectively, not shown in Fig. 1), as well as OH and H_2O masers and compact 20 μm sources (IRS 4, IRS 5) (Harris and Wynn-Williams 1976; Colley 1980; Forster *et al.* 1978; Genzel and Downes 1977; Wynn-Williams, Becklin, and Neugebauer 1972). Werner *et al.* (1980) have made a detailed far-IR study of the W3 core. Observations both of molecular lines from neutral gas and recombination lines from ionized and partially ionized gas show a strong velocity gradient across the core (Dickel *et al.* 1980; Brackmann and Scoville 1980; Jaffe and Wilson 1981). Brackmann and Scoville (1980) have interpreted this gradient as a result of rotation.

We present here a 35'' resolution, 400 μm continuum map of the core of W3. Submillimeter (SMM) continuum emission traces the dust column density in warm, dense clouds. Westbrook *et al.* (1976) mapped the W3 region at 1 mm with a 1' beam, but their map suffers from significant contamination of the thermal dust emission by free-free emission from the ionized gas. At 400 μm , however, the dust emission is much stronger than the free-free emission over most of the region.

¹Visiting Astronomer at the Infrared Telescope Facility which is operated by the University of Hawaii under contract to the National Aeronautics and Space Administration.

II. OBSERVATIONS

We observed W3 in 1979 November and 1981 March with the NASA 3 m Infrared Telescope Facility (IRTF) and the University of Chicago f/35 SMM photometer (Whitcomb, Hildebrand, and Keene 1980). Scans of Mars show that the 20 mm focal plane aperture used for the observations resulted in an approximately Gaussian beam with a full width at half-maximum of 35''. A low-frequency pass filter (Whitcomb and Keene 1980) and diffraction by the field optics and the telescope fixed the limits of the instrumental spectral passband at 300 μm and 800 μm . The flux-weighted mean wavelength for the line-of-sight water vapor during the observations (0.4–1.3 mm) was 400 μm . We mapped the region by making a series of beam-switched measurements at points separated by 20''. The chopping secondary mirror of the IRTF gave a beam separation of 300'' north-south. The map consists of approximately 100 grid points. We derived the flux density scale from comparisons of the flux toward W3 IRS 5 and the flux toward the peak of OMC-1 which is known to $\pm 30\%$ (Keene, Hildebrand, and Whitcomb 1982, hereafter KHW). The W3 IRS 5 peak flux density is $250 \pm 100 \text{ Jy}$. The relative flux at different points in the map is accurate to approximately $\pm 5\%$ of the peak value.

III. RESULTS

Figure 2 shows the distribution of 400 μm continuum radiation in W3. The heavy lines are intensity contours which we have normalized to the intensity measured toward W3 IRS 5. The light line shows the outlines of the mapped region, and the left and right plus signs represent the positions of W3 IRS 5 and IRS 4 (Wynn-

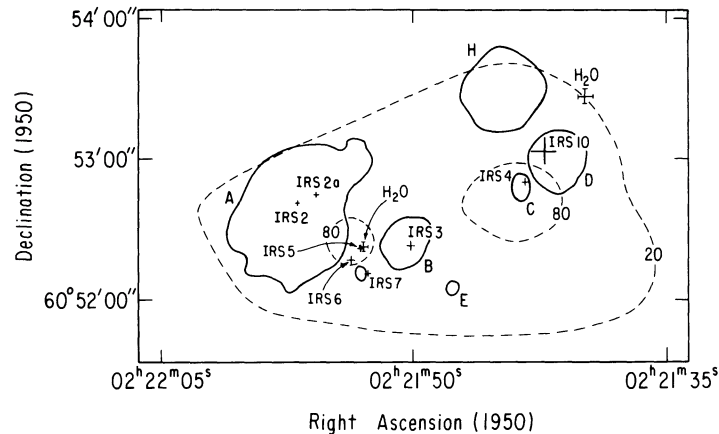


FIG. 1.—A schematic diagram of the W3 cloud core (adapted from Colley 1980). The solid lines outline the radio continuum sources labeled A, B, etc., following the nomenclature of Harris and Wynn-Williams (1976). The plain plus signs show the positions of the $20 \mu\text{m}$ sources, labeled IRS 1, IRS 2, etc., following Wynn-Williams, Becklin, and Neugebauer (1972), and the barred plus signs show the H_2O maser positions (Forster *et al.* 1978; Genzel and Downes 1977). The radio continuum sources W3F and W3M (not shown) lie near IRS 7 and IRS 5 respectively. The dashed lines show the 20% and 80% contours of the $400 \mu\text{m}$ map.

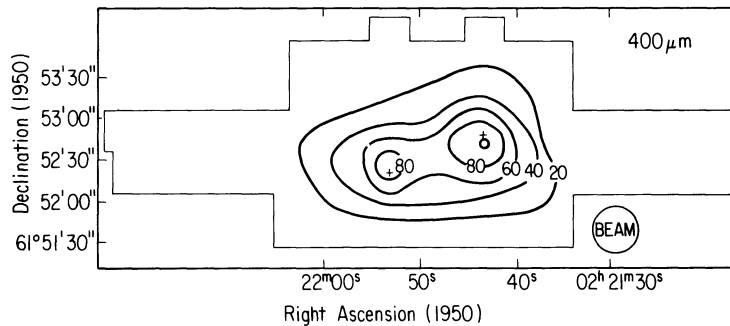


FIG. 2.—A $400 \mu\text{m}$ map of W3. The flux density contours are normalized to 100 at the position of the eastern peak. The positions of IRS 4 and IRS 5 are marked with plus signs near the western and eastern peaks respectively. The flux density in a single $35''$ beam centered at IRS 5 is $250 \pm 100 \text{ Jy}$.

Williams, Becklin, and Neugebauer 1972) respectively. The SMM peak at IRS 4 is approximately 5% brighter than the peak at IRS 5. The circle at the lower right shows the half-power size of the beam. Figures 3 (*upper*) and 3 (*lower*) show declination cuts through the SMM peaks at IRS 4 and IRS 5 (*dashed lines*). The solid lines indicate the beam profile normalized to the peak of each source.

We summarize our main SMM results below and explain them further in the remainder of this section.

1. The core consists of two clumps whose peaks lie approximately $75''$ ($= 2 \times 10^{18} \text{ cm}$) apart (more than two full beamwidths; Fig. 2).

2. The positions of the two peaks agree to within the errors ($\pm 10''$) with the positions of the two most compact, strong $20 \mu\text{m}$ sources, IRS 4 and IRS 5 (Wynn-Williams, Becklin, and Neugebauer 1972; Fig. 2).

3. If the radial dependence of dust density is Gaussian, the peak at IRS 4 has a diameter of about $50''$, and the peak at IRS 5 has a diameter of about $30''$ (Fig. 3).

4. The $400 \mu\text{m}$ peak optical depth toward IRS 5 is approximately 0.044. This corresponds to a visual extinction $A_v \sim 260$. The extinction toward IRS 4 is approximately 180.

5. The total mass of gas and dust in the cloud core is approximately $900 M_\odot$, divided roughly equally between the two clumps.

6. The peak molecular hydrogen density (consistent with the assumptions in the third result above) is approximately $2.8 \times 10^5 \text{ cm}^{-3}$ for IRS 5 and approximately 1.1×10^5 for IRS 4.

a) Optical Depth and Visual Extinction

We derive the $400 \mu\text{m}$ optical depth along the line of sight to W3 IRS 5 from the relationship

$$\tau_{400 \mu\text{m}} = \frac{\Omega_S + \Omega_B}{\Omega_S} \frac{S_\nu}{B_\nu(T) \Omega_B} \approx 0.44, \quad (1)$$

where Ω_S is the source solid angle (taken to be that of a

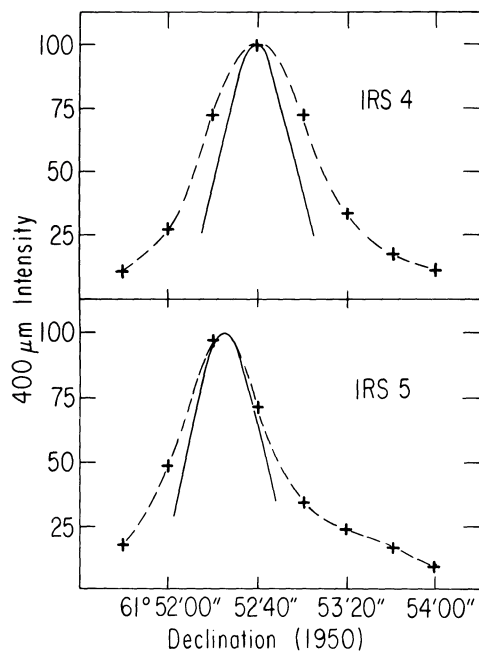


FIG. 3.—A $400\ \mu\text{m}$ map of north-south cross cuts through (upper) W3 IRS 4 and (lower) W3 IRS 5. The vertical size of the cross indicates the noise at each position, and the solid lines show the measured beam profile normalized to the two peaks.

$30''$ Gaussian) and Ω_B is the beam solid angle. Since the source sizes are of the same order as the beam size, we have no detailed information about the source shapes. We have assumed a Gaussian source distribution since this makes the derivation of sizes, optical depths, and densities mathematically tractable. We quote peak optical depth and density derived under this assumption as representative of the physical conditions in the sources. Actual densities could be considerably higher if the dust and gas distributions are shaped more like power laws than Gaussian distributions (Westbrook *et al.* 1976). S_v is the flux into a beam centered on IRS 5, and $B_v(T)$ is the Planck function where we have used an average dust temperature of 50 K (Werner *et al.* 1980). We have used the value determined by Whitcomb *et al.* (1981) for the ratio of 250 nm to $125\ \mu\text{m}$ optical depth which implies $A_v/\tau_{400\ \mu\text{m}} \sim 6000$ to obtain $A_v \sim 260$ along a line of sight through IRS 5. Becklin *et al.* (1978) derive the relation $A_v/\tau_{9.7\ \mu\text{m}} \approx 8 \pm 3$. Willner (1977) has measured the optical depth of the $9.7\ \mu\text{m}$ silicate feature to be 7.6, implying $A_v \sim 60$. Similarly, his results imply $A_v \sim 50$ for IRS 4. Earlier, higher values for the ratio $A_v/\tau_{9.7\ \mu\text{m}}$ (~ 14 , Gillett *et al.* 1975; 24 ± 4 , Rieke 1974) imply A_v values of 100–180 for these two sources. Although large systematic errors arise in a comparison of A_v derived from the $9.7\ \mu\text{m}$ feature and A_v derived from SMM results, such a comparison for W3 IRS 4 and IRS 5 implies that they are deeply embedded in the cloud that emits the SMM radiation.

b) Mass

If $N(\text{H} + \text{H}_2) = 1.9 \times 10^{21} A_v$ (Bohlin, Savage, and Drake 1978), we derive from the work of Whitcomb *et al.* (1981, see also Hildebrand 1983)

$$N(\text{H} + 2\ \text{H}_2) = 1.2 \times 10^{25} \tau_{400} \text{ atoms cm}^{-2}. \quad (2)$$

Integrating over the entire SMM map (above the 20% contour), we derive a mass of $900 M_\odot$ for the cloud if 25% of the mass is in helium and heavier elements. This mass is consistent with the values derived from the dust optical depths at $50\ \mu\text{m}$ (Werner *et al.* 1980) and 1 mm (Westbrook *et al.* 1976).

We can use the measured velocity gradient across the W3 core (Dickel *et al.* 1980; Brackmann and Scoville 1980) to calculate a mass under the assumption that the gradient is a result of rotation. If we assume that the core consists of two lumps of equal mass $M/2$ separated by distance $2a$, we have

$$M = \frac{4av_r^2}{G}. \quad (3)$$

For $a = 0.4\ \text{pc}$ and $v_r = 2\ \text{km s}^{-1}$, we obtain $M = 1300 M_\odot$. Although the mass obtained in this way is very sensitive to both the assumed source geometry and the assumed rotational velocity, the good agreement with the mass we derive from the SMM observations indicates that the low-velocity gas in the core could be in rotational equilibrium.

c) Density

For an optically thin isothermal source with a Gaussian density distribution and an angular full width to half-maximum ϑ , the peak molecular volume density n_{H_2} is related to the column density N_{H_2} by

$$n_{\text{H}_2} = \sqrt{\frac{4 \ln 2}{\pi}} \frac{N_{\text{H}_2}}{\vartheta d}, \quad (4)$$

which is approximately 2.8×10^5 toward the peak at W3 IRS 5 for $\vartheta = 30''$ and $d = 2\ \text{kpc}$. This is an order of magnitude smaller than the value we derive from the data of KHW for the inner $30''$ of OMC-1, $n_{\text{H}_2} \sim 2.5 \times 10^6$. If we could move Orion to a distance of 2 kpc, however, the map of KHW implies that it would have a mean density in the inner $35''$ of 1.2×10^5 . This suggests that the peak densities in W3 may be as much as an order of magnitude higher than the density we derive with a $35''$ beam if it is not a Gaussian source as modeled here.

IV. DISCUSSION

a) Are the H II Regions in Pressure Equilibrium with the Molecular Cloud?

The high, neutral densities suggested by using the OMC-1 results of KHW to extrapolate the current re-

sults to smaller scale sizes lead naturally to the question of confinement of the ionized regions. Could H II regions be in pressure equilibrium with dense shells of neutral gas around them? In the optically thin case, we can express the density of a dust shell as a function of the radius, r , of the enclosed H II region, the solid angle subtended by the H II region plus shell, Ω , and the observed flux from the shell, S_ν :

$$n_{\text{H}_2} = \frac{1.2 \times 10^{25}}{2r} \frac{3}{4} \left[\frac{(1 + \Delta)^2}{(1 + \Delta)^3 - 1} \right] \frac{S_\nu}{\Omega B_\nu(T)}, \quad (5)$$

where Δ is the shell thickness expressed as a fraction of r , and the hydrogen column density is related to $\tau_{400 \mu\text{m}}$ as in equation (2). If the dust temperature is 50 K and the distance to the source is 2 kpc, we can reexpress equation (5) in terms of the angular diameter size of the H II region, ϑ , in arc seconds:

$$n_{\text{H}_2} = 2.8 \times 10^7 \vartheta^{-3} \frac{S_\nu(\text{Jy})}{(1 + \Delta)^3 - 1} \text{ cm}^{-3}. \quad (6)$$

If we now *assume* the H II regions ($T_e = 8 \times 10^3$ K) are in pressure equilibrium with the surrounding neutral gas in the shell ($n_{\text{H}_2} T_{\text{gas}} = 2n_e T_e$; $T_{\text{gas}} = T_{\text{dust}} = 50$ K), we can place upper limits on the thickness of the neutral shells by assuming that they emit less than the observed amount of 400 μm flux in the map from the area including the H II region. Under these assumptions, the thickness of the shell around the largest H II region, W3A ($n_e = 4800$, $\vartheta = 59''$), must be less than 0.2% of its radius, while the shell around the ultracompact source W3F ($n_e = 22,000$, $\vartheta = 2''.5$; Colley 1980), near W3 IRS 7, must have a thickness less than 3 times its inner radius. The postulated W3A shell is clearly too thin to impede the expansion of the H II region. Examining all of the H II regions, we find that any shells dense enough to be in pressure equilibrium with the ionized gas must be insufficiently thick to prevent expansion in all sources except the two most compact, W3F and W3M (near W3 IRS 5). Inspection of the radio continuum maps of the remaining H II regions (Colley 1980) shows that all of the *ionized* regions (which also have the form of shells) have a broken appearance as though ionized gas were streaming out through holes in the surrounding molecular shells (Tenorio-Tagle 1979; Bodenheimer, Tenorio-Tagle, and Yorke 1979). Thus, the pressure inside the ionized region may be lowered allowing the sources to expand only slowly into the cloud, even if the cloud densities are not higher than a few 10^5 cm^{-3} over large

areas. The two ultracompact sources, W3F and W3M, are possibly either very young or simply have been unable to ionize enough material to eat their way out of the denser clumps in which they formed and so are now held in pressure equilibrium with the remaining small clumps of very dense neutral material.

b) SMM Emission and the Youngest Luminous Stars

The two near-IR sources closest to the SMM peaks are both strong, compact, 20 μm emitters (Wynn-Williams, Becklin, and Neugebauer 1972) with deeper silicate features than any of the other sources in the W3 region (Willner 1977). While both have nearby, compact H II regions (Colley 1980), the ratio of 20 μm to radio continuum flux density (250 for IRS 4 and 7×10^4 for IRS 5) is considerably larger than the normal value of 25–60 for 20 μm emission from dust inside H II regions heated by resonantly scattered Lyman- α (Genzel *et al.* 1982). W3 IRS 5 is coincident to $\pm 2''$ with a strong H₂O maser emission center (Forster *et al.* 1978). It has the high 3.5–12 μm color temperature that seems to be characteristic of pre-main-sequence objects directly associated with H₂O maser emission (e.g., Genzel *et al.* 1982; Downes *et al.* 1981). W3 IRS 4 is marginally smaller than and spatially displaced from its nearby H II region W3C (Wynn-Williams, Becklin, and Neugebauer 1972; Colley 1980). Its 20 μm to radio continuum flux ratio therefore may be much larger than the value quoted above. It also may be a pre-main-sequence object, although its luminosity must be considerably lower than that of IRS 5 (Werner *et al.* 1980).

The large 9.7 μm optical depths toward IRS 4 and IRS 5 and the considerably lower value of this quantity toward other nearby 20 μm sources in W3 imply that a considerable fraction of the extinguishing dust lies close to the near-IR sources. This dust also may be responsible for the small structure in our submillimeter maps, that is, for the peaks in the overall distribution at IRS 4 and IRS 5. These peaks, therefore, may be directly associated with the youngest infrared sources in the region.

We thank Drs. R. Genzel, D. A. Harper, and E. E. Becklin for helpful comments. This work was supported in part by NASA grant NAG-W-4. Jocelyn Keene and S. E. Whitcomb acknowledge support from the Fannie and John Hertz Foundation. J. K. was also supported by the National Science Foundation under grant SPI 79-14841, and S. E. W. was also supported by grant SPI 79-14911.

REFERENCES

- Becklin, E. E., Matthews, K., Neugebauer, G., and Willner, S. P. 1978, *Ap. J.*, **220**, 831.
 Bodenheimer, P., Tenorio-Tagle, G., and Yorke, H. W. 1979, *Ap. J.*, **233**, 85.
 Bohlin, R. C., Savage, B. D., and Drake, J. F. 1978, *Ap. J.*, **224**, 132.
 Brackmann, E., and Scoville, N. Z. 1980, *Ap. J.*, **242**, 112.
 Colley, D. 1980, *M.N.R.A.S.*, **193**, 495.

- Dickel, H. R., Dickel, J. R., Wilson, W. J., and Werner, M. W. 1980, *Ap. J.*, **237**, 711.
 Downes, D., Genzel, R., Becklin, E. E., and Wynn-Williams, C. G. 1981, *Ap. J.*, **244**, 869.
 Forster, J. R., Welch, W. J., Wright, M. C. H., and Baudry, A. 1978, *Ap. J.*, **221**, 137.
 Genzel, R., Becklin, E. E., Wynn-Williams, C. G., Moran, J. M., Reid, M. J., Jaffe, D. T., and Downes, D. 1982, *Ap. J.*, **255**, 527.
 Genzel, R., and Downes, D. 1977, *Astr. Ap. Suppl.*, **30**, 145.
 Gillett, F. C., Jones, T. W., Merrill, K. M., and Stein, W. A. 1975, *Astr. Ap.*, **45**, 77.
 Harris, S., and Wynn-Williams, C. G. 1976, *M.N.R.A.S.*, **174**, 649.
 Hildebrand, R. H. 1983, *Quart. J.R.A.S.*, **24**, in press.
 Jaffe, D. T., and Wilson, T. L. 1981, *Ap. J.*, **246**, 113.
 Keene, J., Hildebrand, R., and Whitcomb, S. 1982, *Ap. J. (Letters)*, **252**, L11 (KHW).
 Rieke, G. H. 1974, *Ap. J. (Letters)*, **193**, L81.
 Tenorio-Tagle, G. 1979, *Astr. Ap.*, **71**, 59.
 Werner, M. W., et al. 1980, *Ap. J.*, **242**, 601.
 Westbrook, W. E., Werner, M. W., Elias, J. H., Gezari, D. Y., Hauser, M. G., Lo, K. Y., and Neugebauer, G. 1976, *Ap. J.*, **209**, 94.
 Whitcomb, S. E., Gatley, I., Hildebrand, R. H., Keene, J., Sellgren, K., and Werner, M. W. 1981, *Ap. J.*, **246**, 416.
 Whitcomb, S. E., Hildebrand, R. H., and Keene, J. 1980, *Pub. A.S.P.*, **92**, 863.
 Whitcomb, S. E., and Keene, J. 1980, *Appl. Optics*, **19**, 197.
 Willner, S. P. 1977, *Ap. J.*, **214**, 706.
 Wynn-Williams, C. G., Becklin, E. E., and Neugebauer, G. 1972, *M.N.R.A.S.*, **160**, 1.

R. H. HILDEBRAND: Enrico Fermi Institute, University of Chicago, 5630 Ellis Avenue, Chicago, IL 60637

D. T. JAFFE: Space Sciences Laboratory, University of California, Berkeley, CA 94720

JOCELYN KEENE: Department of Physics, California Institute of Technology, 320-47, Pasadena, CA 91125

S. E. WHITCOMB: Division of Physics, Mathematics and Astronomy, California Institute of Technology, 130-33, Pasadena, CA 91125